

Enhancement of Mixed Conductivity in Ni-based YSZ cermet for SOFC Applications

V. Mohanta and B. K. Roul*

Institute of Materials Science, Planetarium Building, AcharyaVihar, Bhubaneswar-751013, Odisha, India

Abstract

YSZ/Ni cermet has been successfully synthesized using a simple and cost effective combustion process from an aqueous solution containing $ZrO(NO_3)_2 \cdot 6H_2O$, $Y(NO_3)_3 \cdot 6H_2O$, $Ni(NO_3)_2 \cdot 6H_2O$ and urea followed by H_2 reduction. The cermet was examined using X-ray diffraction (XRD), scanning electron microscopy (SEM), and X-ray photoelectron spectroscopy (XPS) techniques. Processed powder of YSZ/NiO was found to be in crystalline form with homogeneous mixture of YSZ and NiO phases. Dielectric constant and dielectric loss are seen to be increased sharply in the high temperature region, which is expected to be onset of dipolar relaxation phenomena due to the presence of oxygen vacancies in the composite. Dielectric properties, thus studied have been corroborated with the conduction mechanism. With increasing temperature, the mobility of oxygen vacancies becomes higher irrespective of frequencies. The decrease in dielectric constant and loss factor with increase in frequency at a given temperature suggests the dynamic interaction of oxygen vacancies and oxide ion pairs in the crystal lattice. The conductivity of YSZ/NiO composite and calculated activation energies suggests a mixed conductivity of ionic and electronic conduction. The microstructure of YSZ/Ni cermet shows a well-defined porous network, which is necessary for the enhancement of electrochemical performance of the anode. The electrical conductivity as a function of temperature of YSZ/Ni cermet shows the metallic behavior. All these behavior find potential use as ideal anodic materials for SOFC applications.

Keywords: Combustion synthesis, YSZ/Ni cermet, Dielectric properties, Mixed conductivity, SOFC

1. INTRODUCTION

Solid oxide fuel cell (SOFC) is one of the most advanced environmental friendly, electrochemical devices for generating electricity directly from chemical energy with high efficiency [1]. The principal advantages of SOFC, which make it most promising energy converter over other types of fuel cells are fuel flexibility, design modularity, high efficiency, environmental friendly, and long term stability [2,3].

Mixed ionic-electronic conductors (MIECs) which exhibit both ionic and electronic conductivity have a wide range of applications, such as gas separating membranes, water electrolysis, electro-catalytic reactors, and electrodes in solid oxide fuel cells [4, 5]. The mixed conductors help to improve the electrochemical activities since electrochemical reactions take place not only at the electrode/electrolyte interface, but also in the whole surface area of the MIECs electrode [6]. MIECs which are compatible with electrolytes are promising candidate materials for SOFC electrodes.

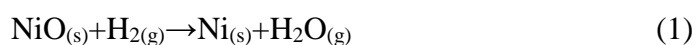
The mixed conduction can be achieved from the single phase materials (like cerium oxide and some rare earth manganite) or from the mixture of ionic and electronic conductors [5]. High electronic and significant oxygen ion conductivity has been reported in perovskite-based LnMO_3 ($\text{Ln}=\text{La, Sr, Y, \dots}$, $\text{M}=\text{Co, Mn, Cr, \dots}$) oxides in zirconia-based SOFC [7]. Zirconia based mixed conducting oxides are regarded as advanced electrode material due to their good chemical and thermal compatibility with the zirconia electrolyte. Most of these are single phase materials that can be fabricated using transition metal ions into yttria-stabilized zirconia (YSZ) [8]. Some others like ceria [9], titania [7], terbia [10], and iron [11] induce electronic conduction in YSZ. However, some of enhanced properties have been attributed in a two phase mixture rather than single phase MIECs [12]. The relative magnitude of electronic and ionic conductivity can also be easily tailored by mixing two phases. Such MIECs like $\text{ZrO}_2\text{-In}_2\text{O}_3$ [13], $\text{CeO}_2\text{-NiO}$ [14] have been reported. The possibility of tailoring the properties to optimize the processing parameters for a specific application is the main challenge of the MIEC composite [5]. Apart from above, more details of electronic and ionic migration mechanism with the temperature and frequency are required to understand the electrode performance [15].

In our present study, the SOFC anode is the cermet YSZ/Ni, produced by the reduction of the precursor composite YSZ/NiO [16]. Both the cermet and the oxide precursor are MIEC composite. The advantages of selecting present material is that, the electronic conductor NiO and ionic conductor YSZ, both are stable at high temperatures, their solubility in each other's phase is limited, and the electrical conductivity of NiO is easily controlled by doping. In addition, this leads to enlarge the electrochemical reaction zone, enhance the electrode stability, adherence to the electrolyte, provides mechanical durability, and adjusts the thermal expansion coefficients [17].

In this paper, we report a detailed electrical and micro-structural characterization of the YSZ/Ni cermet prepared by combustion route and followed by hydrogen reduction to produce high performance anode for possible SOFC applications.

2. EXPERIMENTAL PROCEDURE

Ni-doped YSZ composite powder has been produced by combustion synthesis using urea as fuel. Nitrate salts; Ni(NO₃)₂·6H₂O (Aldrich, 99.999%), Y(NO₃)₃·6H₂O (Aldrich, 99.8%) and ZrO(NO₃)₂·6H₂O (Aldrich, 99.0%) were taken as metal precursor. These materials in the required stoichiometric proportions were calculated as per propellant chemistry based on thermo-chemical concepts, wherein the total oxidizing and reducing valences of the precursors and the fuel is zero [18]. To improve the crystallinity, the amount of urea was taken twice the theoretical amount [2]. The above nitrates and urea were mixed in a silica basin and dissolved in distilled water. The solution is heated on a hot plate. After evaporation of water a thick, viscous gel was obtained. The basin was then introduced into a furnace, preheated at 600^oC, where the combustion reaction took place. High temperature reactions were revealed by sudden release of fumes, resulting in dry, fragile foam or loose agglomerates. These agglomerates were converted to a fine powder with mild manual crushing by agate mortar. The pellets of size 8 mm in diameter and 2 mm in thickness were obtained applying a uniaxial pressure of 200 MPa. The green pellets were sintered at 1350 ^oC for 5 hours with a heating rate of 3 ^oC per minute. NiO was reduced back to Ni metal under flowing 10% H₂/90% Ar reducing atmosphere at 800 ^oC for 5 hours. The reaction with reducing atmosphere is explained through following chemical reaction mechanism:



The phase composition and crystal structure of as prepared composite and cermets were investigated by Bruker (D8) XRD with Cu K α ($\lambda=1.5406 \text{ \AA}$) radiation, EVO-60 (JEISS) SEM and XPS by ESCALAB high performance electro spectrometer. Dielectric and conductivity study for various frequencies and temperatures were performed by a microprocessor controlled programmable LCR meter bridge (QuadTech).

3. RESULT AND DISCUSSIONS

3.1 XRD analysis

XRD patterns of YSZ/NiO composite powder synthesized by the combustion process and reduced YSZ/Ni cermet pellets are shown in Fig 1.

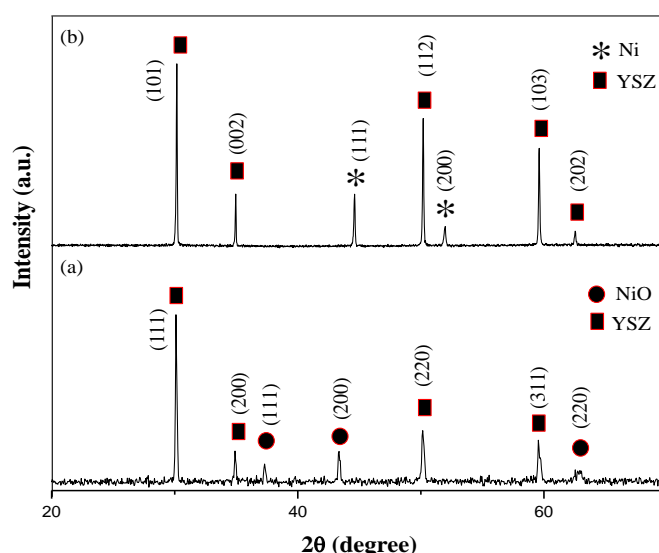


Fig. 1 XRD pattern of (a) YSZ/NiO composite and (b) YSZ/Ni cermet.

Rietvelt analysis, as well as the search test program developed by us [19] were used for refinement of XRD patterns.

Two crystalline phases, NiO and YSZ were observed for the YSZ/NiO composite in Fig 1(a). No peak corresponding to metallic Ni or any other undesirable phases were found within the detection limits of XRD. It was observed from the XRD refinement that both YSZ and NiO are in the cubic phase (space group: Fm3m). The cubic phase of YSZ and NiO has been indentified from (111) and (200) peaks respectively [20]. The lattice parameters observed for YSZ is 5.139 Å (JCPDS file no. 030-1468), while that for NiO is 4.176 Å (JCPDS file no. 04-0835). XRD pattern of reduced sample in Fig 1(b) reveals complete reduction of NiO to Ni, since there is no peak corresponding to NiO. From refinement it was observed that YSZ is in tetragonal phase (space group: P42/nmc) and Ni is in the cubic phase (space group: Fm3m). The lattice parameters observed for YSZ are $a=b=3.63$ Å, $c=5.139$ Å (JCPDS file no. 070-4434) and for Ni is 3.5157 Å (JCPDS file no. 070-0989).

Crystallite size of NiO, YSZ and Ni phases was determined from their highest intensity peaks using Scherrer's formula [21]:

$$A = K\lambda / \beta \cos\theta \quad (2)$$

where, K is shape factor, λ is the wavelength of the X-ray beam (1.5406 Å) used, θ is

the angle between the incident beam and reflecting plane, and β is the full width at half maximum (FWHM) of the X-ray diffraction peaks.

Crystallite size of YSZ and NiO in YSZ/NiO composite powder were found to be 84 nm and 22 nm respectively. However, crystallite sizes of YSZ and Ni in YSZ/Ni cermet were found to be 128 nm and 73 nm respectively. This grain growth is due to high temperature sintering and reduction [22].

3.2 Scanning Electron Microscopy

SEM micrographs of YSZ/NiO composite sintered at 1350 °C and reduced YSZ/Ni cermet are shown in Fig 2. The micrograph reveals a distinct grain growth with well defined grains separated by grain boundaries. Interlinking between grains along with the presence of scanty voids is also observed in Fig 2(a).

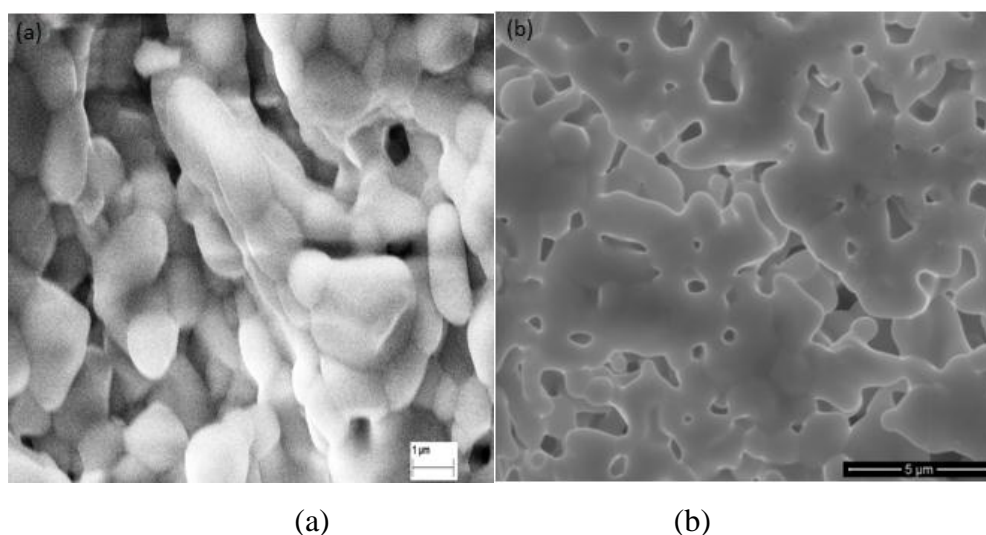


Fig. 2 SEM micrograph of (a) YSZ/NiO composite sintered at 1350 °C for 5 hr and (b) reduced YSZ/Ni cermet.

The surface morphology significantly depends upon the concentration of different phases. Again, dissolution of different phases depends upon the ionic radius, and in our case, the ionic radius of Ni^{2+} is small in comparison to both the Zr^{4+} and Y^{3+} . The mismatch between ionic radius leads to non-uniform grain morphology observed in SEM micrograph [20]. Highly dense grain morphology has been noticed with the size of grain ranging from the submicron to several microns. The average grain sizes of grains seen in SEM micrograph and crystallite size calculated from XRD differ somehow due to the formation of agglomerates of small size grains at higher sintering

temperature. However, in XRD, there may be single crystallite, which is a part of a grain separated from a defect as a coherent domain, smaller in size from SEM, wherein the complete grain is visualized with higher size [22, 23].

Following reduction of the NiO, the SEM micrograph in Fig 2(b) of YSZ/Ni cermet reveals significant porous structure with respect to YSZ/NiO sintered composite (Fig 2(a)) which is highly favorable to maximize the electrochemical reaction by enhancing the triple phase (Ni-YSZ-gas) boundary, thereby improving anodic properties [18].

3.3 X-ray Photoelectron Spectroscopy

From XPS studies of YSZ/NiO composite, we observed two main peaks, one near 870 eV and another near 857 eV in Fig 3(a) corresponding to $2p_{1/2}$ and $2p_{3/2}$ oxidation states of Ni [24]. The observed binding energy of Ni $2p_{3/2}$ peak is higher than the metallic Ni $2p_{3/2}$ (852.3 eV), indicates Ni is in positively charged. Again, the difference between above peaks is nearly 13 eV. This reveals that Ni is in +2 oxidation state [24, 25]. A satellite peak near 864 eV is also observed.

Broad and slightly asymmetric natures of peaks in Fig 3 (b) are observed in the XPS spectrum of O (1s). The Peak near 530 eV (peak 1) and 532 eV (peak 2) may be attributed to the lattice oxygen and the near-surface oxygen respectively [24]. The diffusion of oxide ion via vacancies forms oxygen ion-vacancy pair [26]. The mobility of oxygen ion from one vacancy site to another forms a transient dipole. On application of external electric field to such a dipole, the charge transports within the crystal lattice may be affected due to induced dipolar orientation [26].

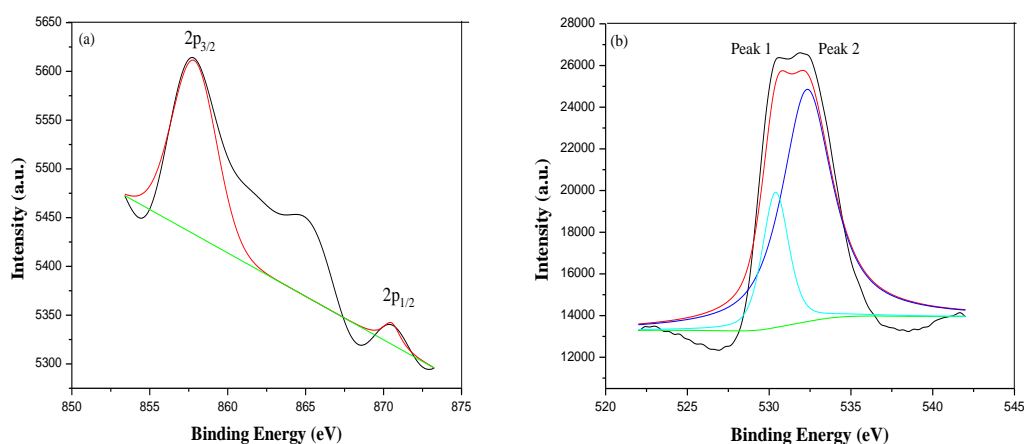


Fig. 3 XPS spectrum of (a) Ni(2p) and (b) O(1s) in YSZ/NiO sintered sample.

3.4 Dielectric behavior

In Fig 4 (a) the value of dielectric constant in the low temperature region is very low and almost constant, indicates the absence of any significant dipolar interaction under the action of applied electric field [26]. However, it increases sharply in the high temperature region. Again, it decreases with the increase of applied frequency (Fig 4.b). Dielectric polarization in non-conductors is mainly due to (i) electronic polarizability and (ii) orientational polarizability. At low frequency, electronic polarizability and orientational polarizability contribute to dielectric constant, whereas; dielectric constant just results from the electron displacement polarization at high frequency [27]. There is a random diffusion of charge carriers via activated hopping, which leads to an increase in the dielectric response in the high temperature region [18]. Oxygen vacancies are the key factors for observation of such dielectric behavior [18].

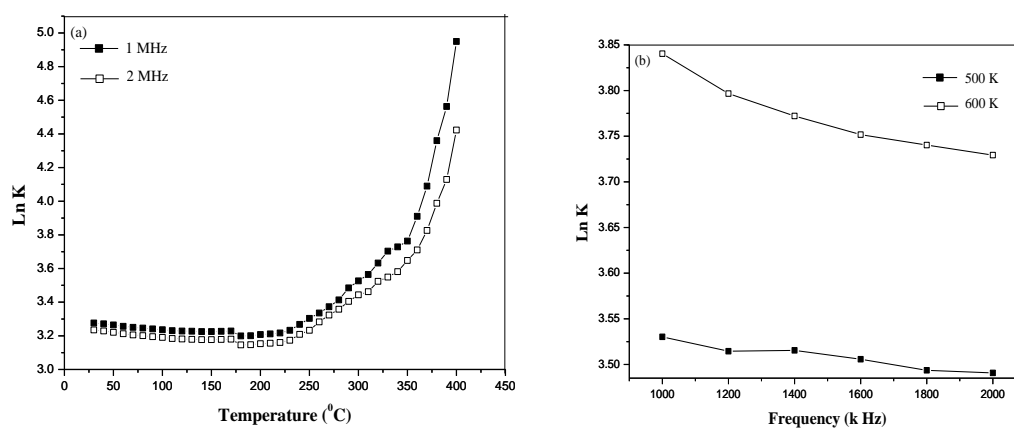


Fig. 4 (a) Temperature and (b) Frequency dependent behavior of dielectric constant in YSZ/NiO sintered composite.

The temperature dependence of dielectric constant and dielectric loss at frequency 1 MHz for YSZ/NiO sample is shown in Fig 5(a). It is observed from figure that both are remained temperature independent in the low temperature region. There is a rapid increase of both the parameters with increase in the temperature. The sharp increase of dielectric loss in a high temperature region may be attributed to the increased mobility of charge carriers due to defects or vacancies in the sample [28]. However, in Fig 5(b), both dielectric constant and dielectric loss have higher values at lower frequency than that with rising frequency, indicating the presence of dipolar relaxation phenomena.

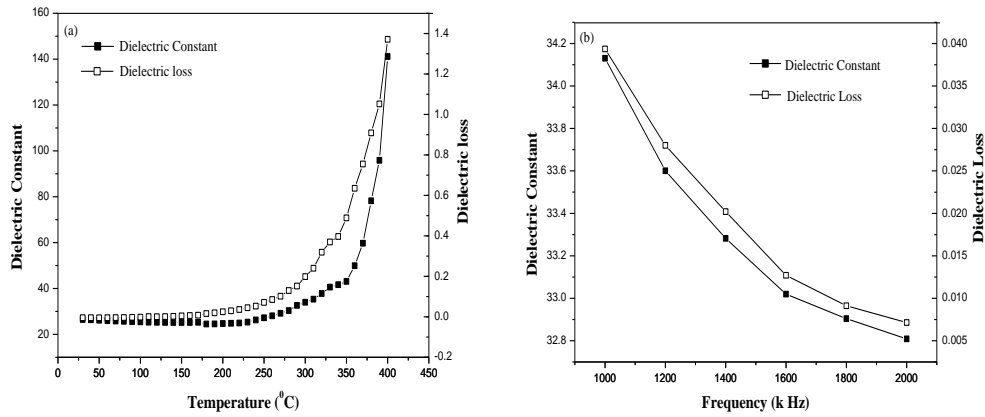


Fig. 5 (a) Temperature versus Dielectric constant and Dielectric loss at frequency 1 MHz for YSZ/NiO sintered sample (b) Frequency versus Dielectric constant and Dielectric loss at temperature 500 K for YSZ/NiO sintered sample.

3.5 Conductivity

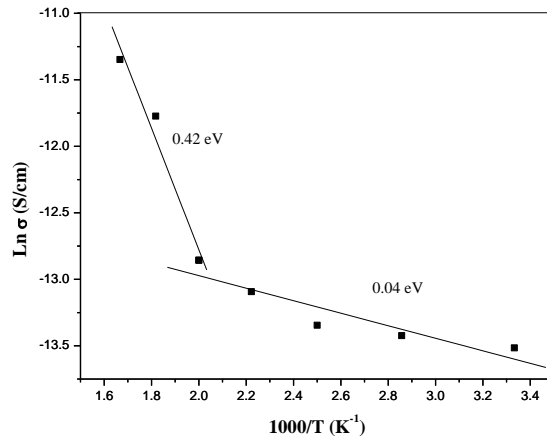


Fig. 6 Arrhenius plot for conductivity of sintered YSZ/NiO composite at frequency 2 MHz.

Fig 6 shows the Arrhenius plot for electrical conductivity of YSZ/NiO composite at frequency 2 MHz. The activation energy for the conduction process is calculated from the slope of the line, according to Arrhenius equation [29];

$$\sigma = A \exp (-E_a/K_B T) \tag{3}$$

where, A is the pre-exponential factor, E_a is the activation energy, K_B is the

Boltzmann constant and T is the absolute temperature. There is a mixed ionic-electronic conductivity [30] observed in YSZ/NiO composite.

In the high temperature region, conduction takes place due to holes (anion vacancies) as well as electrons, whereas in the low temperature region it is mainly due to electrons only [31]. It is because; holes are activated at high temperature since more activation energy is required for them than electrons. The activation energies corresponding to low (27⁰C-227⁰C) and high (227⁰C-327⁰C) temperature region, respectively are 0.04 eV and 0.42 eV. Hopping process of electrons between ions of different valences results smaller activation energy in low temperature [32].

Above result and discussion envisaged two different transport mechanism for electrical conductivity: (i) short range transport mechanism, originates from hopping process of charge carriers (holes and/or electrons) between different ions in localized states around Fermi level at low temperature, resulting lower activation energy; and (ii) long range transport mechanism, originates from thermally activated charge carriers into extended state at higher temperature, resulting higher activation energy [33]. The electrical properties of composite depend not only on the electrical properties of each phase but also are strongly influenced by micro-structural and morphological studies, since anode materials provide percolation paths for electrons, oxygen ions and gases. So, the electrochemical performance is closely related to the electrode microstructure [34]. Though, some models like percolation and effective media have been applied to study the electrical properties, no analytical solution for this problem has yet been found [35]. However, electro-chemical reaction completely depends on the nature of the charge carriers and the dependence of the electrical transport properties on the microstructure, temperature, and oxygen partial pressure of MIEC composites.

I-V characteristic of YSZ/Ni cermet anode shown in Fig 7 is linear, suggesting metallic behavior. The electrical conductivity as a function of temperature (200⁰C-500⁰C) at 2 MHz frequency has been shown in Fig 8. The conductivity decreases with increasing temperature, also suggests metallic behavior. This implies proper Ni-to-Ni contact network present in YSZ/Ni cermet. Generally the electrochemical reaction in SOFC takes place at the TPB where electrons are liberated by reactions. Electrons, thus, liberated are required to be transported through a metallic Ni phase. For this reason, Ni-to-Ni contact proximity inside anodic material should have a compatible microstructure with a uniform and contiguous distribution of metallic Ni phase.

In our present observations, cermet of YSZ/Ni with significant porosities (Fig 2.b) promoting metallic behavior (Fig 7 & 8) and mixed conduction at high temperature (Fig 6) are indicatives of Ni-to-Ni connectivity network within the bulk cermet.

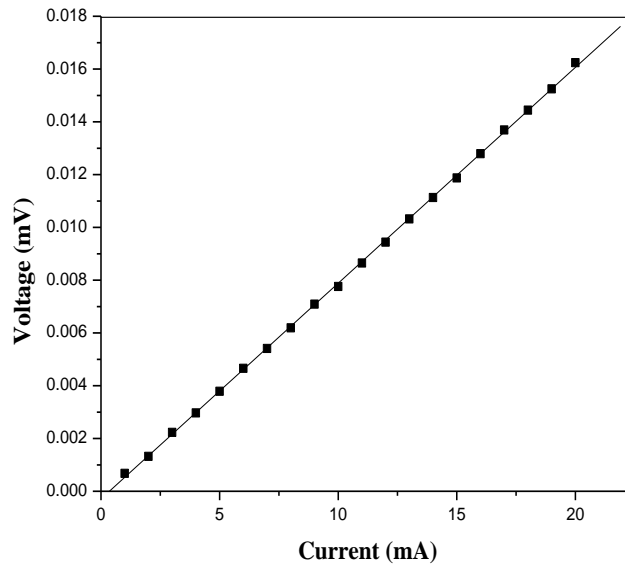


Fig. 7 I-V characteristic of YSZ/Ni cermet.

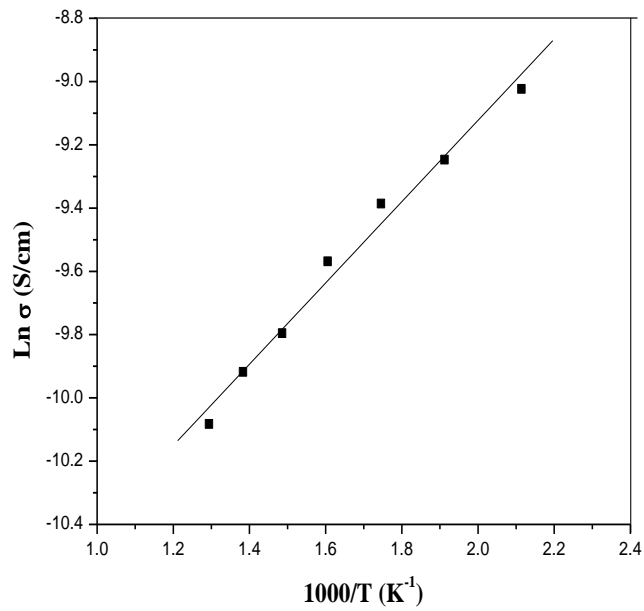


Fig. 8 Electrical conductivity of YSZ/Ni anode cermet as a function of temperature.

4. CONCLUSIONS

The enhancement of both micro-structural and electrical properties of Ni-based YSZ cermet suggests the suitability of our preparation method for fabrication of SOFC anode material. Mixed (oxygen ion and electronic) conduction mechanism is observed with increasing temperature. Reduction of YSZ/NiO composite under hydrogen atmosphere (10% H₂/90% Ar) yielded a porous YSZ/Ni cermet. Cermet porosity promotes an interconnected Ni-to-Ni network, which is necessary for effective electrochemical performance in the anode. It is expected that Ni-to-Ni metallic phase network in YSZ along with the porous channel increase the TPB needed for the enhanced electrochemical property. Contiguous Ni-to-Ni network also provides good electrical conductivity. The electrical conductivity as a function of temperature shows also a metallic behavior which promotes the requirement of anodic performance required for SOFC applications.

ACKNOWLEDGEMENTS

Author, V. Mohanta, acknowledges to the Director, Institute of Materials Science, Bhubaneswar, Odisha, India for providing experimental facilities to carry out this research work and Institute of Minerals and Materials Technology, Bhubaneswar for the synthesis of the sample. The authors are also very much thankful to Institute of Physics, Bhubaneswar, India for the SEM and XPS measurements. The authors would also like to thank the Department of Physics, Utkal University, Bhubaneswar, India for carrying out XRD measurements.

REFERENCES

- [1] Mohebbi, H., Ebadzadeh, T., and Hesari, F. A., 2009, "Synthesis of nanocrystalline NiO-YSZ by microwave-assisted combustion synthesis," *Power Technol.*, 188(3), pp. 183-186.
- [2] Ribeiro, N. F. P., Souza, M. M. V. M., Neto, O. R. M., Vasconcelos, S. M. R., and Schmal, M., 2009, "Investigating the microstructure and catalytic properties of Ni/YSZ cermets as anodes for SOFC applications," *Appl. Catalysis A: General*, 353(2), pp. 305-309.
- [3] Singh, G., and Singh, K. L., 2012, "Characterization of NiO-YSZ nanocomposite synthesized by combustion method," *Int. J. for Sci. and Emerg. Technol.*, 3(1), pp. 1-8.
- [4] Tuller, H.L., 1992, "Mixed ionic electronic conduction in a number of fluorite and pyrochlor compounds," *Solid State Ionics*, 52(1-3), pp. 135-146.
- [5] Reiss, I., 2003, "Mixed ionic-electronic conductors-material properties and

- applications,” *Solid State Ionics*, 157(1-4), pp. 1-17.
- [6] Adler, S. B., Lane, J. A., and Steele, B. C. H., 1996, “Electrode kinetics of porous mixed conducting oxygen electrodes,” *J. Electrochem. Soc.*, 143 (11), pp. 3554-3564.
- [7] Lion, S. S., and Worrell, W. L., 1989, “Electrical properties of novel mixed-conducting oxides,” *Appl. Phys. A*, 49(1), pp. 25-31.
- [8] Huang, X. J., and Weppner, W. J., 1996, “Characteristics of transition metal oxide doping of YSZ: structure and electrical properties,” *Chem. Soc. Faraday Trans.*, 92 (12), pp. 2173-2178.
- [9] Cales, B., and Baumard, J. F., 1980, “Electrical properties of the ternary solid solutions $(\text{ZrO}_{21-x}\text{-CeO}_2 \text{ }_x)_{0.9} \text{-Y}_2\text{O}_3 \text{ }_{0.1}$ ($0 \leq x \leq 1$),” *Rev. int. hautes Temper. Refract.*, Fr., 17, pp.137-147.
- [10] Han, P., and Worell, W. L., 1995, “Mixed (oxygen ion and p-type) conductivity in yttria stabilized zirconia containing terbia,” *J. Electrochem. Soc.*, 142 (12), pp. 4235-4246.
- [11] Matsui, N., and Takigawa, M., 1990, “Impedance spectroscopy on YSZ with iron oxide as additive,” *Solid State Ionics*, 40-41 (2), pp. 926-928.
- [12] Wu, Z., and Liu, M., 1997, “Modelling of ambipolar transport properties of composite mixed ionic-electronic conductors,” *Solid State Ionics*, 93, pp. 65-84.
- [13] Gauckler, L. J., and Sasaki, K., 1995, “Ionic and electronic conductivities of homogeneous and heterogeneous materials in the system $\text{ZrO}_2 \text{—In}_2\text{O}_3$,” *Solid State Ionics*, 75, pp. 203-210.
- [14] Tare, V. B., Mehrotra, G. M., and Wagner, J. B., 1986, “Electrical transport in NiO-CeO₂ mixtures,” *Solid State Ionics*, 18-19(2), pp. 747-750.
- [15] Martines, R. F., Brant, M. C., Domingues, R. Z., Paniago, R. M., Sapag, K., and Matencio, T, 2009, “Synthesis and characterization of NiO-YSZ for SOFCs,” *Mater. Res. Bull.*, 44(2), pp. 451-456.
- [16] Kawashima, T., and Hishinuma, M., 1996, “Analysis of Electrical Conduction Paths in Ni/YSZ Participate Composites Using Percolation Theory,” *Mater. Trans.*, 37, pp. 1397-1403.
- [17] Sarantaridis, D. , and Atkinson, A., 2007, “Redox Cycling of Ni-Based Solid Oxide Fuel Cell Anodes: A Review,” *Fuel cells*, 7(3), pp. 246-258.
- [18] Priyatham, T., and Bauri, R., 2010, “Synthesis and characterization of nanocrystalline Ni-YSZ cermet anode for SOFC,” *Mater. Char.*, 61(1), pp. 54-58.

- [19] Roul, B. K., 2001, "Modulated structural characteristics and microwave properties of spray pyrolyzed superconducting BCSCO," *J. of Supercond.*, 14(4), pp. 531-537.
- [20] Singh, K. L., Kumar, A., Singh, A. P., and Sekhan, S. S., 2008, "Microwave processing: A potential technique for preparing NiO-YSZ composite and Ni-YSZ cermet," *Bull. Mater. Sci.*, 31(4), pp. 655-664.
- [21] Xi, X., Abe, H., and Naito, M., 2014, "Effect of composition on microstructure and polarization resistance of solid oxide fuel cell anode NiOYSZ composite made by co-precipitation," *Ceram. Int.*, 40(10), pp. 16549-16555.
- [22] Steil, M. C., Thevenot, F., and Kleitz, M., 1997, "Densification of Ytria-Stabilized Zirconia: Impedance Spectroscopy Analysis," *J. Electrochem. Soc.*, 144(1), pp. 390-398.
- [23] Gaber, A., Abdel-Rahim, M. A., Abdel-Latief, A. Y., and Abdel-Salam, M. N., 2014, "Influence of Calcination Temperature on the Structure and Porosity of Nanocrystalline SnO₂ Synthesized by a Conventional Precipitation method," *Int. J. of Electrochem. Sci.*, 9(1), pp. 81-95.
- [24] Das, S. K., Mishra, R. N., and Roul, B. K., 2014, "Magnetic and ferroelectric properties of Ni doped BaTiO₃," *Solid State Commun.*, 191, pp. 19-24.
- [25] Xu, Q., Chen, W., and Yuan, R., 2001, "XPS analysis of Ni and Oxygen in single-sintered SrTiO₃ multifunction ceramic," *J. Mater. Sci. Technol.*, 17(5), pp. 535-537.
- [26] Pandey, N., Thakur, A. K., and Choudhary, R. N. P., 2008, "Studies on dielectric behaviour of an oxygen ion conducting ceramic CaMnO_{3-δ}," *Indian J. of Eng. & Mater. Sci.*, 15(2), pp. 191-195.
- [27] Das, S. K., Mishra, R. N., and Roul, B. K., 2014, "Diluted magnetic ferroelectric effect in BaTi_{0.9}Hf_{0.05}Co_{0.05}O₃ ceramic," *Appl. Phys. A*, 116(4), pp. 1897-1903.
- [28] Yadav, V. S., Sahu, D. K., Singh, Y., and Dhubkarya, D. C., 2010, "The effect of frequency and temperature on dielectric properties of pure poly vinylidene fluoride (PVDF) thin films," *Proceedings of International Conference of Engineers and Computer Scientist, Hongkong, EMECS Vol 3*.
- [29] Sudha, L. K., Roy, S., and Uma Rao, K., 2014, "Evaluation of Activation Energy (E_a) Profiles of Nanostructured Alumina Polycarbonate Composite Insulation Materials," *Int. J. of Mater. Mech. and Manuf.*, 2(1), pp. 96-100.

- [30] Park, Y. M., and Choi, G. M., 1999, "Mixed ionic and electronic conduction in YSZ-NiO composite," *J. of Electro Soc.*, 146(3), pp. 883-889.
- [31] Manikandan, M., and Venkateswaran, C., 2014, "Effect of high energy milling on the synthesis temperature, magnetic and electrical properties of barium hexagonal ferrite," *J. of Magn. Mater.*, 358-359, pp. 82-86.
- [32] Gabal, M. A., Abdel-Daiem, A. M., Angari, Y. M. A., and Ismail, I. M., 2013, "Influence of Al-substitution on structural, electrical and magnetic properties of Mn-Zn ferrites nanopowders prepared via the sol-gel auto-combustion method," *Polyhedron*, 57, pp. 105-111.
- [33] Senturk, E., Koseoglu, Y., Sasmaz, T., Alan, F., and Tan, M., 2013, "RC circuit and conductivity properties of $Mn_{0.6}Co_{0.4}Fe_2O_4$ nanocomposite synthesized by hydrothermal method," *J. Alloys Compd.*, 578, pp. 90-95.
- [34] Zhu, W.Z., and Deevi, S. C., 2003, "A review on the status of anode materials for solid oxide fuel cells," *Mater. Sci. and Eng. A*, 362(1-2), pp. 228-239.
- [35] Uvarov, N. F., 2000, "Estimation of Composites Conductivity Using a General Mixing Rule," *Solid State Ionics*, 136-137, pp. 1267-1272.